



POLİTEKNİK DERGİSİ

JOURNAL of POLYTECHNIC

ISSN: 1302-0900 (PRINT), ISSN: 2147-9429 (ONLINE)

URL: <http://dergipark.org.tr/politeknik>



Determination of the construction material for phononic band gap structures by tribological performance

Fonon bant aralığı gösteren yapılar için yapı malzemesinin tribolojik performansla belirlenmesi

Yazar(lar) (Author(s)): Paşa YAMAN¹, Erol TÜRKEŞ², Osman YÜKSEL³

ORCID¹: 0000-0003-2079-5800

ORCID²: 0000-0002-9601-7119

ORCID³: 0000-0001-9492-1756

To cite to this article: Yaman P., Türkeş E. ve Yüksel O., “Determination of the construction material for phononic band gap structures by tribological performance”, *Journal of Polytechnic*, 28(1): 27-34, (2025).

Bu makaleye şu şekilde atıfta bulunabilirsiniz: Yaman P., Türkeş E. ve Yüksel O., “Determination of the construction material for phononic band gap structures by tribological performance”, *Politeknik Dergisi*, 28(1): 27-34, (2025).

Erişim linki (To link to this article): <http://dergipark.org.tr/politeknik/archive>

DOI: 10.2339/politeknik.1424547

Determination of the Construction Material for Phononic Band Gap Structures by Tribological Performance

Highlights

- ❖ AISI 303, 304, 316L and 420 specimens are compared in term of dry and lubricated wear tests.
- ❖ AISI 420 stainless steel is found to be the highest wear resistant specimen for dry and lubricated tests.
- ❖ In the lubricated condition, abrasive wear is the dominant wear mechanism.
- ❖ Higher viscosity lubrication blocks the flow of the lubricant and semi-dry friction occurs.
- ❖ Lower viscosity lubricant provided lower wear compared to higher viscosity lubricant.

Graphical Abstract

303, 304, 316L, and 420 grade stainless steels are evaluated for applying in the phononic band gap structures by their tribological performance. Dry and lubricated wear tests are applied, and it is revealed that mixed (adhesive and abrasive) wear behavior is obtained in the dry friction, while abrasive wear is observed for lubricated friction.



Figure. Lubricated wear of the specimen and optical micrograph

Aim

The aim of the study is to determine the construction material of the inertial amplification induced phononic band gap periodic structures considering their tribological performances on supports.

Design & Methodology

The material determination process is conducted according to the tribological performance of stainless steel specimens in the dry and lubricated wear tests.

Originality

The wear behavior can change the operation properties of isolators and supports, but the tribological interaction between these periodic structures and supports is not studied yet in the literature.

Findings

It is found that viscosity is a crucial factor in the frictional interaction of lubricated wear. High viscosity lubricant can be an adverse property by lowering wear resistance of the material.

Conclusion

The lubrication lowers the wear related damage on the contact surface, however, the viscosity needs to be considered for a long service life.

Declaration of Ethical Standards

The author(s) of this article declare that the materials and methods used in this study do not require ethical committee permission and/or legal-special permission.

Determination of the Construction Material for Phononic Band Gap Structures by Tribological Performance

Research Article / Araştırma Makalesi

Paşa YAMAN^{1*}, Erol TÜRKES¹, Osman YÜKSEL¹

¹Kırklareli University, Faculty of Engineering, Department of Mechanical Engineering, 39010, Kırklareli, Türkiye

(Geliş/Received : 23.01.2024 ; Kabul/Accepted : 10.04.2024 ; Erken Görünüm/Early View : 30.04.2024)

ABSTRACT

This study investigates the tribological performances of commonly used stainless steel alloys (303, 304, 316L, and 420) to determine their suitability as construction materials for periodic structures designed for inertial amplification induced phononic band gap vibration isolators. Stainless steel alloys are extensively employed in engineering structures due to their ability to withstand large stresses and exhibit excellent cyclic loading properties. In this study, stainless steel specimens are examined by dry and lubricated wear test conditions. 420 stainless steel showed highest wear resistant properties for dry and lubricated conditions. Two grades of lubricants are compared in terms of viscosities, and it is revealed that higher viscosity blocked the flow of the lubricant so that semi-dry friction occurred. Low viscosity lubricant enabled less material removal due to friction. 420 stainless steel yielded the lowest wear rate by 2.7-1.3 times for dry, by 4.0~2.8 times for low viscosity lubrication, and by 1.19~1.33 times for high viscosity lubrication conditions. In terms of coefficient of friction, 420 stainless steels showed higher results about 12.7~15.8% related to its structural properties.

Keywords: Elastic metamaterial, inertial amplification, stainless steel, wear, lubrication.

Fonon Bant Aralığı Gösteren Yapılar İçin Yapı Malzemesinin Tribolojik Performansla Belirlenmesi

ÖZ

Bu çalışmada, yaygın olarak kullanılan paslanmaz çelik alaşımlarının (303, 304, 316L ve 420) atalet artırımının tetiklediği fonon bant aralığı gösteren titreşim yalıtıcıları olarak tasarlanan periyodik yapılar için yapı malzemesi olarak uygunluklarını belirlemek amacıyla tribolojik performansları incelenmiştir. Paslanmaz çelik alaşımları, büyük gerilmelere dayanma yetenekleri ve iyi döngüsel yükleme özellikleri sergilemeleri nedeniyle mühendislik yapılarında yaygın olarak kullanılmaktadır. Bu çalışmada paslanmaz çelik numuneler kuru ve yağlamalı aşınma testi koşullarında incelenmiştir. Çalışmada 420 paslanmaz çeliğin, kuru ve yağlı koşullar için en yüksek aşınma direncini gösterdiği görülmüştür. İki tür yağlayıcı viskozite açısından karşılaştırıldığında, yüksek viskoziteli yağlayıcının akışı bloke ettiği ve dolayısıyla yarı kuru sürtünme oluşturduğu ortaya çıkmıştır. Düşük viskoziteli yağlayıcının, sürtünme nedeniyle daha az malzeme kaybına sebep olduğu gözlemlenmiştir. 420 paslanmaz çelik diğer numunelere kıyasla, kuru sürtünme için 2,7~1,3 kat, düşük viskoziteli yağlama için 4,0~2,8 kat ve yüksek viskoziteli yağlama için 1,19~1,33 kat ile en düşük aşınma oranını vermiştir. Sürtünme katsayısı açısından 420 paslanmaz çelik, yapısal özelliklerine bağlı olarak yaklaşık %12,7~15,8 oranında daha yüksek sonuçlar göstermiştir.

Anahtar Kelimeler: Elastik metalmalzeme, atalet artırımı, paslanmaz çelik, aşınma, yağlama.

1. INTRODUCTION

Stainless steel alloys are among the most utilized and manufactured structural materials in the engineering field [1,2]. Thus, when considering engineering structures which can both carry loads and deform elastically, these are the material of natural choice [3]. Since, they can withstand large stresses and they have great cyclic loading properties without failure, stainless steel alloys are also used in vibration isolation applications as the construction material. Traditionally, this is achieved via mass-spring type vibration isolators [4-6]. On the other hand, recently, as an innovative approach, periodic structures constructed with stainless steel alloys can be utilized as efficient vibration isolators, as well [7-8].

Periodic structures that can inhibit vibration transmission for a certain frequency range are called elastic metamaterials or phononic band gap structures [9]. These structures are formed by periodically end to end attaching a repetitive building block called the unit cell throughout the entire frame. In the literature, there exist multiple studies that were conducted on periodic structures constructed with various stainless steel alloys, which aim to achieve vibration mitigation from the source to the target system [10-13]. In these works, a phenomenon called Bragg scattering [14] is utilized to attain vibration isolation for some frequency bands.

Besides, vibration isolation frequency bands can be created via a different method called inertial

*Corresponding Author

e-posta : pasa.yaman@klu.edu.tr

amplification [15], as well. In the literature, there are various experimental studies which investigate the vibration isolation properties of stainless steel constructed periodic structures of this type [16-18]. Since, periodic vibration isolators are stationed between the target and the source structures, their connections are achieved via supports. Moreover, the isolators can be replaced time to time, hence it is not practical to weld the connection positions of the periodic vibration isolators to the supports. As a result, roller boundary conditioned supports can be a suitable option for the design.

When roller boundary conditions are considered, the interaction occurred as a result of continuous vibration between the base structures (i.e., target or source) and the isolator will lead to wear type of deformation. The extent of this wear behavior can alter the service life of both the isolator and the supports in a negative manner. Therefore, a designer should also take into account the wear behavior in construction material selection of a periodic vibration isolator structure. However, the interaction between these periodic structures and the supports has never been studied yet.

To that end, in this study, various readily available stainless steel specimens are evaluated based on their

tribological performances to determine the construction material of the inertial amplification induced phononic band gap periodic structures. 303, 304, 316L and 420 stainless steel alloys are selected as the material of construction for the periodic structure [19-21]. Moreover, in the experimental wear studies dry, lubrication with low viscosity fluid and lubrication with high viscosity fluid cases are considered. This work's outcomes will provide foresight to researchers on determining the proper construction material of phononic band gap structures for varied operation conditions in terms of tribological aspect.

2. MATERIAL AND METHOD

2.1. Specimens and Lubricants

AISI 303, 304, 316L, and 420 stainless steel specimens are selected as substrate material for wear tests. Substrate material for test has a diameter of 30 mm and a thickness of 10 mm. Chemical composition of stainless steels are provided in Table 1. Commercial lubrication agents are determined based on viscosity values, and their properties are tabulated in Table 2. Lubricants of 5W-30 and 80W-90 are abbreviated as L1 and L2, respectively.

Table 1. Chemical composition of stainless steel specimens

	C (%)	Mn (%)	Si (%)	P (%)	S (%)	Cr (%)	Ni (%)	Mo (%)
AISI 303	Max. 0.15	Max. 2.0	Max. 1.0	Max. 0.20	Min. 0.15	17-19	8-10	-
AISI 304	Max. 0.08	Max. 2.0	Max. 0.75	Max. 0.045	Max. 0.03	18-20	8-10	-
AISI 316L	Max. 0.03	2.0	1.0	0.045	0.03	16-18	10-14	2.0-3.0
AISI 420	0.30	Max. 1.0	Max. 1.0	Max. 0.04	Max. 0.03	13.0	-	-

Table 2. Lubricant properties

	Standard	Value (5W-30) "Lubricant 1"	Value (80W-90) "Lubricant 2"
Density, 15°C, kg · L⁻¹	ASTM D4052	0.850	0.890
Viscosity, 40°C, mm² · s⁻¹	ASTM D445	55.6	180

2.2. Test and Characterization Methods

Tribological behavior of specimens are tested using a pin-on-disc tribometer. Sliding wear tests are conducted for 10 N loading and 25 mm·s⁻¹ sliding speed condition

for 200 m at room temperature. Alumina ball is selected as counterpart which has a diameter of 6 mm. Sliding wear tests are applied for dry and lubricated test conditions which is shown in Table 3.

Table 3. Wear test conditions (conditions apply to all specimens)

Specimen	Applied load [N]	Sliding speed [mm · s ⁻¹]	Sliding distance [m]	Wear condition 1	Wear condition 2	Wear condition 3
303						
304	10	25	200	Dry (D)	Lubricated with lubricant 1 (L1)	Lubricated with lubricant 2 (L2)
316L						
420						

2.3. Wear Rate Calculations

Wear rate values (Eq. (2)) are determined based on volume loss calculations (Eq. (1)) [22]. Volume loss (V_{loss}) is calculated based on wear track radius (R), ball radius (r), wear track width (d); and wear rate (W_R) is calculated by means of volume loss, sliding distance (L) and applied load (P).

$$V_{loss} = 2 \pi R \left[r^2 \sin^{-1} \left(\frac{d}{2r} \right) - \left(\frac{d}{4} \right) (4r^2 - d^2)^{0.5} \right] \quad (1)$$

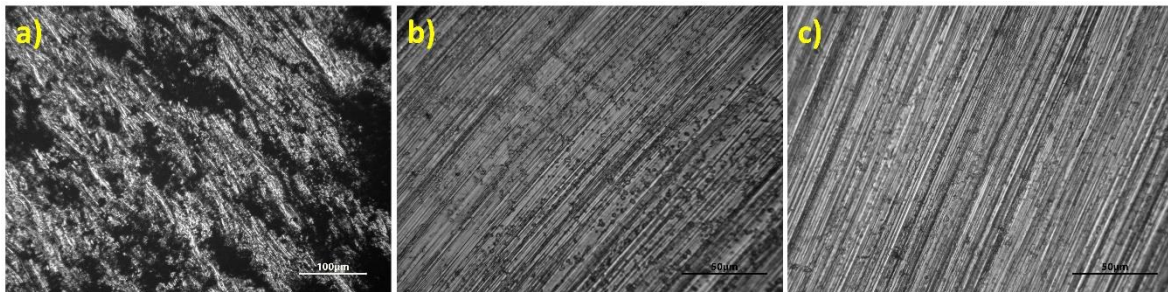
$$W_R = V_{loss} L^{-1} P^{-1} \quad (2)$$

3. RESULTS AND DISCUSSION

3.1. Optical Microscope Investigations

Optical microscope micrographs of 303 steel are illustrated in Figure 1. Harsh adhesive and abrasive wear

mechanisms are observed for dry wear condition (Figure 1a) in which specimens' surface is damaged by abrasive ball and hard particles in the matrix are pulled off. Besides, ploughing mechanism also occurred on the edges of wear track. Debris is distributed over the wear surface so that stuck debris increased the severity of wear behavior. In terms of lubricated test conditions (Figure 1b and 1c), mostly abrasive wear is dominant for both conditions as in [23-24]. Lubrication decreased the strength of wear and smooth surfaces are obtained. Wear resistance of 303 specimen is increased by applying the load in varied test conditions. However, comparing L1 with L2 test condition, deeper grooves can be seen on the surface for the L2 test condition as in Figure 1c.


Figure 1. Optical micrograph of 303 stainless steel after wear test; a) D, b) L1, c) L2

The surface of 304 specimen after subjected to wear tests in different test conditions can be seen in Figure 2. As in 303 steel specimen, a mixed friction regime of adhesive and abrasive behaviors is observed for the dry wear condition. Compared to 303 steel, abrasive wear is more dominant compared to adhesive wear mechanism which can be seen explicitly in Figure 2a. Grooves are formed due to scratches of debris and adhesive wear is overwhelmed [25-27]. A mild adhesive wear can be related with metal removal zones on the wear surface.

Similar to 303 steel, lubricated wear condition eliminated adhesive friction mechanism and solely abrasive wear occurred. The severity of abrasive wear is less in L2 test condition compared to L1 which can be attributed to deeper grooves. 303 and 304 steel specimens have similarities in terms of wear mechanisms and surface observations. This similarity can be attributed to dominant chemical compounds in the matrix. Mostly, closer Cr-Ni composition can be a major factor in the similarity of wear behaviors.

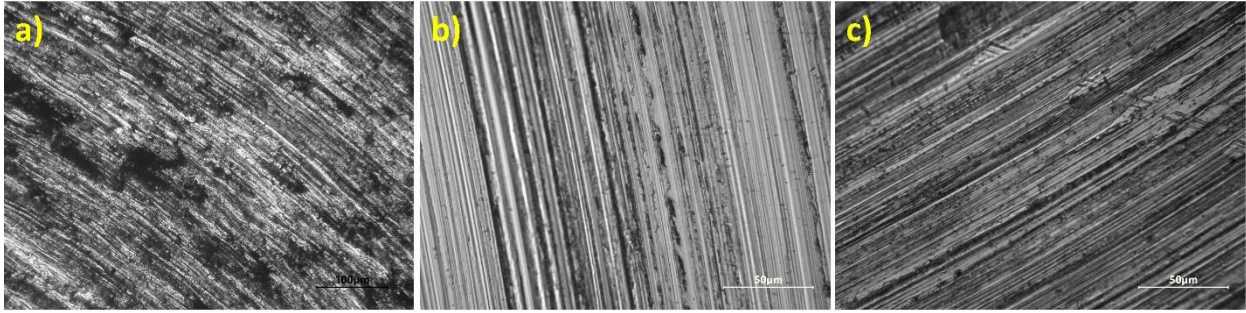


Figure 2. Optical micrograph of 304 stainless steel after wear test; a) D, b) L1, c) L2

Wear track surfaces of 316L steel can be observed after wear test with varied conditions in Figure 3. The operative wear mechanism for dry test condition is adhesive wear. Hard structure of 316L steel resisted against abrasive friction and wear mechanism is occurred as adhesive. Spalling mechanisms and plastic deformation zones can be seen over the surface as

encountered in the literature [28-33]. In the lubricated tests, effects of abrasive friction can be seen on surfaces in Figure 3b and 3c. The lubrication loosened the severity of the friction and abrasive wear related mechanisms are observed such as deep grooves, ploughings, and debris [34] which is a result consistent with the literature, as well.

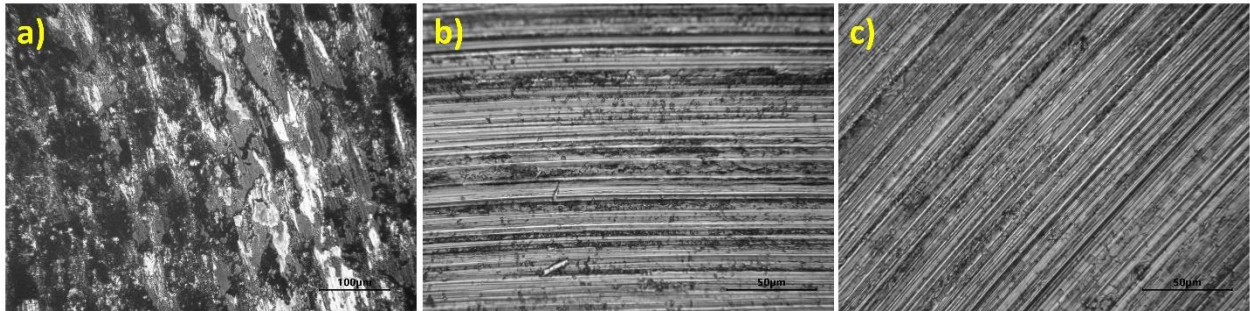


Figure 3. Optical micrograph of 316L stainless steel after wear test; a) D, b) L1, c) L2

The optical micrographs of the surfaces of 420 steel specimens are shown in Figure 4. In Figure 4a, the wear surface of dry-worn specimens is seen in which particularly adhesive wear behavior is observed. The surface is comprised of plastic deformation zones as the

result of removal of loose particles in the matrix and cold-welding of fragments over the surface. In lubricated conditions, wear resistance of the surface is increased, and the friction mechanism is transformed to abrasive wear [35-36].

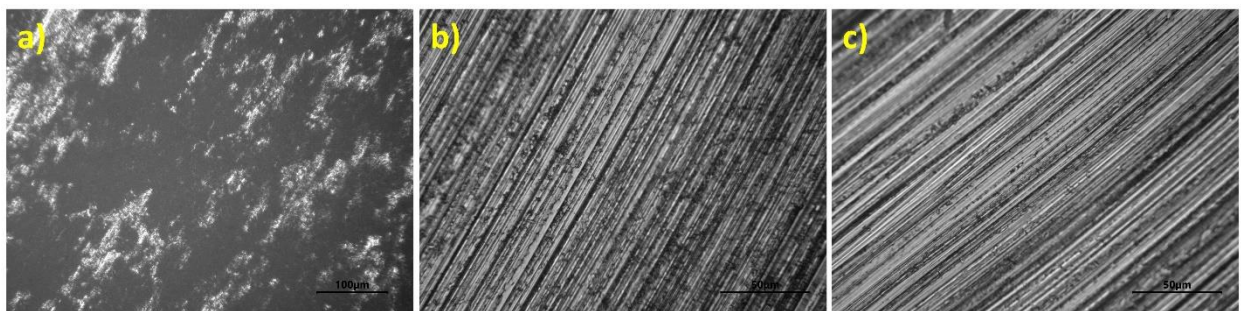


Figure 4. Optical micrograph of 420 stainless steel after wear test; a) D, b) L1, c) L2

In dry wear condition, 303 and 304 steel specimens exhibited a mixed wear regime which is composed of adhesive and abrasive wear behaviors. 316L and 420 steels had particularly adhesive wear behavior on the surface. This can be attributed to the internal structure of

the steels in terms of chemical composition, dominant compounds, surface hardness, and microstructure. 316L and 420 steels have higher surface hardness values compared to 303 and 304 steels. The increase of strength in the mechanical properties revealed higher resistance

against wear and lowered the severity of the friction mechanisms. However, micrograph observations showed that the dominant wear mechanism is abrasive for all lubricated conditions. The lubrication decreased the severity of friction on the wear surfaces, however in lubricant (L2) with high viscosity revealed poor resistance against wear. Deeper grooves are observed for L2 lubricant compared to lower viscosity lubricant (L1). Dry sliding condition enabled the microstructural properties to be dominant in terms of resisting the frictional forces while the lubrication mostly neutralized microstructural characteristics for all specimen in which the surface properties became vital.

3.2. Wear Rate Evaluations

Wear rate calculations are made using wear width values from optical microscope micrographs. Results are calculated based on Eq. (1-2) and given in Figure 5. It can be seen that the wear rate behavior of specimens acts in a similar pattern. Highest wear rate occurred for dry test condition while the lubrication increased the tribological performance so that wear rates significantly decreased. 303 and 304 steels showed the poorest resistance to friction in the specimens for dry wear tests. Applying wear test to 316L and 420 steels, the wear resistance of specimens dropped in almost half and one third, respectively. The increased resistance against wear can be associated with dominant chemical compounds, such as chromium carbide, iron carbide, nickel chromium,

austenitic and martensitic structures, and hardness [37-44]. In the lubricated test condition, lower viscosity (L1) and higher viscosity (L2) lubricants are used, and test results showed that lower viscosity lubricant enabled lower wear rate and higher viscosity lubricant cannot lowered the wear rate. This can be affiliated with poor circulation of lubricant between the wear components. As the viscosity of the lubricant increases, the lubricant poorly circulates between the specimen and abrasive ball so that lubricating film formation is prevented. The poor film formation leads to semi-dry friction between the component [45-46]. This phenomenon is applicable for all specimens, and it is clarified that poor lubricant circulation on the contact surface of components decreases the wear resistance so that the wear rate is increased for tests in L2 lubricant. In the lubricated condition, there is not a significant difference for 303, 304, and 316L specimens in terms of wear rate. However, 420 steel has the highest wear rate resistance for dry, low viscosity and high viscosity lubricants among other specimens which depends on the martensitic microstructure. High strength and low ductile properties enabled enhanced anti-wear characteristics. Wear rate characteristics is also evaluated with wear behavior modes which has a dominant effect in the width and depth of the wear track. Abrasive friction forces damaged the wear surface more compared to adhesive wear for dry sliding. Austenitic microstructure enabled mixed wear mode with a more of abrasive wear while adhesive wear behavior is observed for martensitic microstructure.

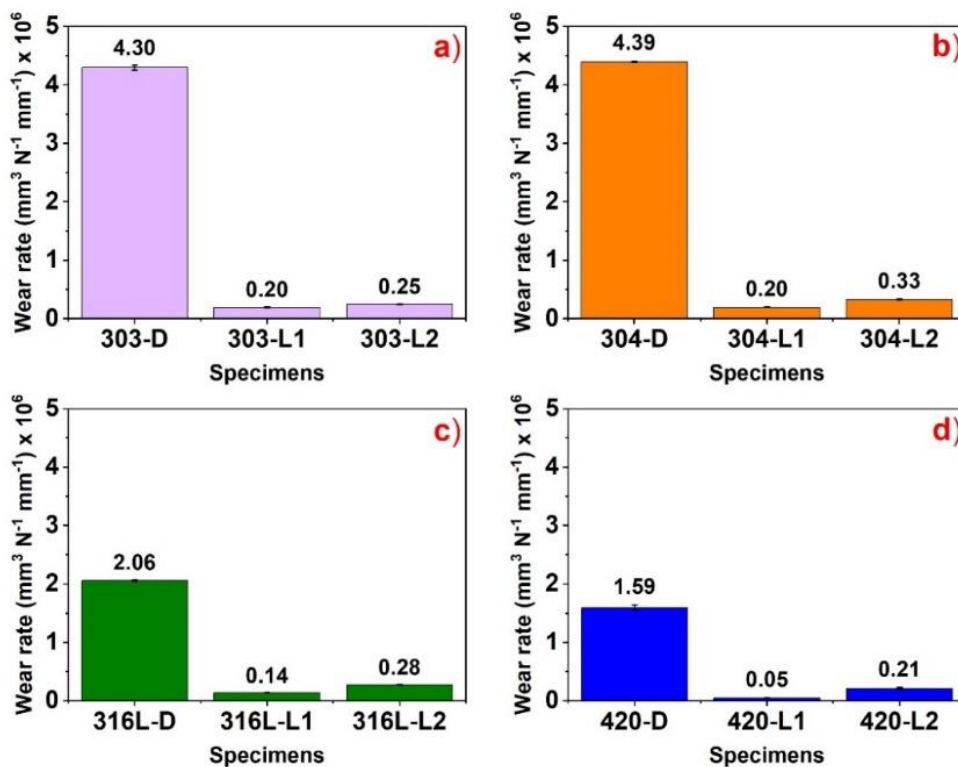


Figure 5. Wear rate values of the specimens

3.3. Coefficient of Friction Evaluations (COF)

The COF values of the specimens are provided in Figure 6. As seen, dry friction provided a fluctuant COF for all steels. COF values of dry sliding wear is quite similar for 303, 304, and 316L steels. However, a higher COF is recorded for 420 steel by 18.8%, 17.2%, and 14.5% in comparison with 303, 304, and 316L, respectively. It is seen that austenitic stainless steels enables a lower COF value compared to martensitic stainless steel. This can be affiliated with body centered tetragonal crystal lattice of 420 steel. High strength and low ductility yielded increased COF values for dry sliding wear in which the martensitic microstructure harshly resisted against the frictional forces. Ductile characteristic of austenitic microstructure absorbed some of the frictional forces so that lower COF values are obtained. On the other hand, the effect of frictional forces is not absorbed, and higher

COF values are yielded by martensitic microstructure. The rigid structure of 420 provided severe reaction against the abrasive ball so that a higher COF is recorded. In lubricated tests, COF values are dropped by almost one fourth compared to dry friction tests. COF values are almost the same for all steel specimens in all test conditions. There is a significant difference between dry and lubricated tests, while similar COF values are obtained among the lubricated tests. Beside wear rate values, it is not possible to evaluate the COF results in terms of lubricated condition. The lubrication of contact surfaces damaged the ability to evaluate the friction properties. Even the lubricants decreased the effect of frictional forces, the microstructure of 420 stainless steel provided the lowest COF values for lubricated test conditions. Lubrication neutralized most of microstructural properties.

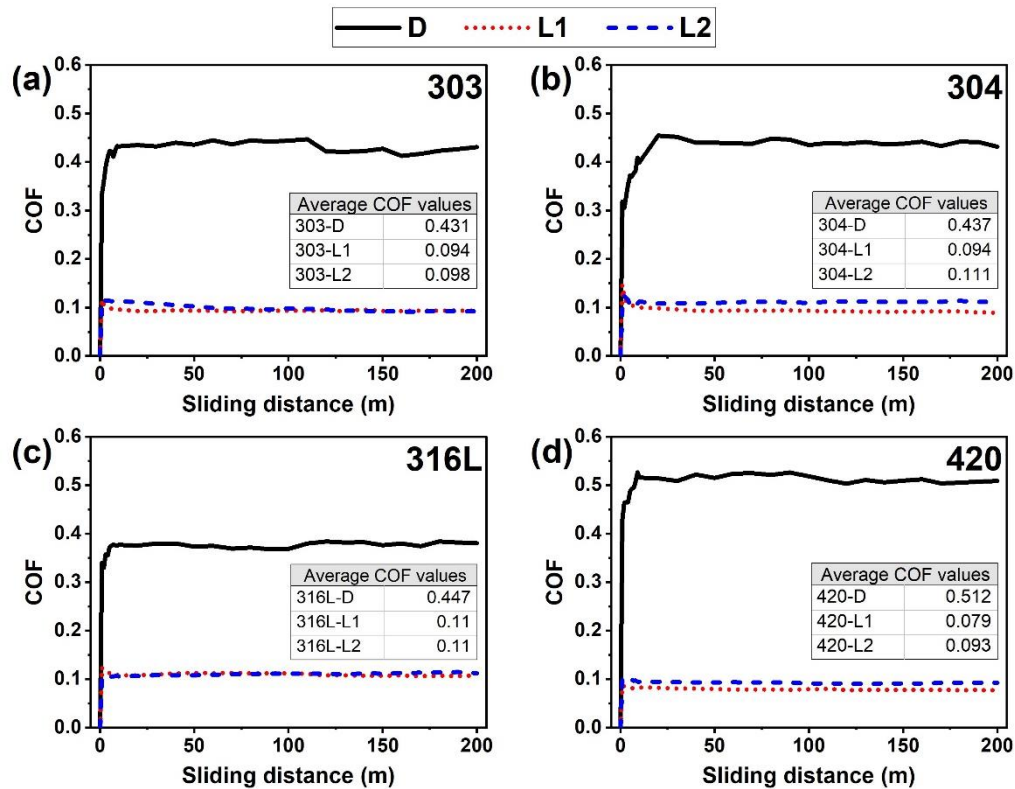


Figure 6. Coefficient of friction values of the specimens.

4. CONCLUSION

In this study, the most used stainless steel specimens are investigated in terms of determination of construction materials for phononic band gap structures. Evaluations are accomplished for tribological performance including dry and lubricated conditions and the major outcomes are provided.

- Optical microscope observations showed that all specimens are worn by mild abrasive behavior for the lubricated tests, while 303 and 304 steels had a mixed wear (adhesive and abrasive), 316L and 420

steels had severe adhesive wear for test in dry environment.

- Wear rate evaluations reported that specimens had the lowest wear resistance in dry tests and the resistance against wear is increased significantly in the lubricated tests. However, the effect of viscosity on the lubrication showed that higher viscosity lubricant cannot flow to the contact surface easily so that semi-dry wear is occurred. Lower viscosity lubricant enabled higher wear resistance compared to higher viscosity lubricant.

- COF values illustrated that lubricated friction enabled smoother wear in the tests, since material's hardness and internal structure properties are crucial for friction of the contact surfaces.

To sum up, considering the wear rate values obtained in this study, 420 stainless steel can be chosen as the construction material of the periodic metamaterial structures and low viscosity lubrication should be employed between the contact surfaces of the periodic structure and the supports.

DECLARATION OF ETHICAL STANDARDS

The author(s) of this article declare that the materials and methods used in this study do not require ethical committee permission and/or legal-special permission.

AUTHORS' CONTRIBUTIONS

Paşa YAMAN: Methodology, investigation, visualization, writing – original draft and revision.

Erol TÜRKES: Investigation, writing – revision, validation.

Osman YÜKSEL: Conceptualization, resources, validation, writing – original draft and revision.

CONFLICT OF INTEREST

There is no conflict of interest in this study.

REFERENCES

- [1] Lo K. H., Shek C. H., and Lai J. K. L., "Recent developments in stainless steels," *Materials Science and Engineering: R: Reports*, 65(4-6): 39-104, (2009).
- [2] Baddoo N. R., "Stainless steel in construction: A review of research, applications, challenges and opportunities," *J Constr Steel Res*, 64(11): 1199-1206, (2008).
- [3] Gardner L., "The use of stainless steel in structures," *Progress in Structural Engineering and Materials*, 7(2): 45-55, (2005).
- [4] Rao S., *Mechanical Vibrations*, Prentice Hall, New Jersey, (2011).
- [5] Inman D., *Engineering Vibration*. Pearson Education, New Jersey, (2014).
- [6] Avallone E. and Baumeister T., *Marks' Standard Handbook for Mechanical Engineers*, McGraw-Hill, New York, (1996).
- [7] Liu L. and Lee H. P., "A Review: Elastic Metamaterials and Inverse Design Methods for Shock and Vibration Mitigation," *Int J Appl Mech*, 13(9): 2150102, (2021).
- [8] Oudich M., Gerard N. J., Deng Y., and Jing Y., "Tailoring Structure-Borne Sound through Bandgap Engineering in Phononic Crystals and Metamaterials: A Comprehensive Review," *Adv Funct Mater*, 33(2): 2206309, (2023).
- [9] Phani A. and Hussein M., *Dynamics of Lattice Materials*, John Wiley & Sons Ltd, West Sussex, (2017).
- [10] Sharma V. and Chandraprakash C., "Fabrication and bandgaps of microscale metallic phononic crystals," *Int J Adv Eng Sci Appl Math*, 15(4): 159-166, (2023).
- [11] Yang C.-L., Zhao S.-D., and Wang Y.-S., "Experimental evidence of large complete bandgaps in zig-zag lattice structures," *Ultrasonics*, 74: 99-105, (2017).
- [12] Lee K. Il, Kim Y. M., Kang H. S., and Yoon S. W., "Acoustic band structures in two-dimensional phononic crystals consisting of periodic square arrays of stainless-steel cylinders in water," *Journal of the Korean Physical Society*, 68(2): 221-226, (2016).
- [13] He C., Zhao H., Wei R., and Wu B., "Existence of complete band gaps in 2D steel-water phononic crystal with square lattice," *Frontiers of Mechanical Engineering in China*, 5(4): 450-454, (2010).
- [14] Sigalas M. M. and Economou E. N., "Elastic and acoustic wave band structure," *J Sound Vib*, 158(2): 377-382, (1992).
- [15] Yilmaz C., Hulbert G. M., and Kikuchi N., "Phononic band gaps induced by inertial amplification in periodic media," *Phys Rev B*, 76(5): 054309, (2007).
- [16] Yuksel O. and Yilmaz C., "Realization of an ultrawide stop band in a 2-D elastic metamaterial with topologically optimized inertial amplification mechanisms," *Int J Solids Struct*, 203: 138-150, (2020).
- [17] Yuksel O. and Yilmaz C., "Shape optimization of phononic band gap structures incorporating inertial amplification mechanisms," *J Sound Vib*, 355: 232-245, (2015).
- [18] Acar G. and Yilmaz C., "Experimental and numerical evidence for the existence of wide and deep phononic gaps induced by inertial amplification in two-dimensional solid structures," *J Sound Vib*, 332(24): 6389-6404, (2013).
- [19] Yıldız U. T., Varol T., Pürçek G., ve Akçay S. B., "A Review on the Surface Treatments Used to Create Wear and Corrosion Resistant Steel Surfaces", *Journal of Polytechnic*, 27(1): 227-236, (2024).
- [20] Gül F., Dilipak H., ve Yamanoğlu O., "Kriyojenik İşlem Yapılmış Soğuk İş Takım Çeliklerinin Abrasif Aşınma Davranışlarının İncelenmesi ve İstatistiksel Analizi", *Politeknik Dergisi*, 24(3): 1129-1135, (2021).
- [21] Ünlüoğlu O. ve Çelik O. N., "Grafit Partiküllerinin Yağ Katkısı Olarak AISI H11 Çeliğinin Sürtünme ve Aşınma Davranışı Üzerine Etkisi", *Politeknik Dergisi*, 25(4): 1495-1503, (2022).
- [22] G99-17, "Standard Test Method for Wear Testing with a Pin-on-Disk Apparatus," *ASTM International*, (2017).
- [23] Mertgenc E., Kesici O. F., and Kayali Y., "Investigation of wear properties of borided austenitic stainless steel different temperatures and times," *Mater Res Express*, 6(7): 076420, (2019).
- [24] Seriacopi V., Fukumasu N. K., Souza R. M., and Machado I. F., "Analysis of Abrasion Mechanisms in the AISI 303 Stainless Steel: Effect of Deformed Layer," *Procedia CIRP*, 45: 187-190, (2016).
- [25] Barcelos M. A., Barcelos M. V., Araújo Filho J. de S., A. Franco Jr. R., and Vieira E. A., "Wear resistance of AISI 304 stainless steel submitted to low temperature plasma carburizing," *REM - International Engineering Journal*, 70(3): 293-298, (2017).
- [26] Ramya Sree K., Keerthi Reddy G., Lakshmi Prasanna G., Saranya J., Anitha Lakshmi A., Swetha M., Vineeth Raj T., and Subbiah R., "Dry sliding wear behavior of treated

- AISI 304 stainless steel by gas nitriding processes,” *Mater Today Proc.* 44: 1406-1411, (2021).
- [27] Fenili C. P., da Rocha M. R., Al-Rubaie K. S., Arnt A. B. C., Angioletto E., and Bernardin A. M., “Effect of sensitization on tribological behavior of AISI 304 austenitic stainless steel,” *International Journal of Materials Research*, 109(3): 234-240, (2018).
- [28] Huang M., Fu Y., Qiao X., and Chen P., “Investigation into Friction and Wear Characteristics of 316L Stainless-Steel Wire at High Temperature,” *Materials*, 16(1): 213, (2022).
- [29] Karabeyoğlu S. S. and Yaman P., “An Experimental Investigation of Martensitic Stainless Steel in Aircraft and Aerospace Industry for Thermal Wear Performance and Corrosion Potential,” *Practical Metallography*, 59(4): 199-215, (2022).
- [30] Karabeyoğlu S. S., Eker B., Yaman P., and Ekşi O., “Effect of boric acid addition to seawater on wear and corrosion properties of ultrashort physical vapor deposited Ti layer on a 304 stainless steel,” *Materials Testing*, 65(4): 467-478, (2023).
- [31] Yaman P., Karabeyoğlu S. S., and Moralar A., “Investigation of mechanical and frictional properties of ulexite and colemanite filled acrylonitrile-butadiene-styrene polymer composites for industrial use,” *Journal of Thermoplastic Composite Materials*, 0(0), Early View, (2023).
- [32] Khan H. M., Yılmaz M. S., Karabeyoğlu S. S., Kısasöz A., and Özer G., “Dry sliding wear behavior of 316 L stainless steel produced by laser powder bed fusion: A comparative study on test temperature,” *Mater Today Commun*, 34: 105155, (2023).
- [33] Özer G. and Kısasöz A., “The role of heat treatments on wear behaviour of 316L stainless steel produced by additive manufacturing,” *Mater Lett*, 327: 133014, (2022).
- [34] Shen M., Rong K., Li C., Xu B., Xiong G., and Zhang R., “In situ Friction-Induced Copper Nanoparticles at the Sliding Interface Between Steel Tribo-Pairs and their Tribological Properties,” *Tribol Lett*, 68(4): 98, (2020).
- [35] Xi Y., Liu D., and Han D., “Improvement of corrosion and wear resistances of AISI 420 martensitic stainless steel using plasma nitriding at low temperature,” *Surf Coat Technol*, 202(12): 2577-2583, (2008).
- [36] Brühl S. P., Charadia R., Sanchez C., and Staia M. H., “Wear behavior of plasma nitrided AISI 420 stainless steel,” *International Journal of Materials Research*, 99(7): 779-786, (2008).
- [37] Boonruang C. and Sanumang W., “Effect of nano-grain carbide formation on electrochemical behavior of 316L stainless steel,” *Sci Rep*, 11(1): 12602, (2021).
- [38] Dadfar M., Fathi M. Karimzadeh H., Dadfar F., M. R., and Saatchi A., “Effect of TIG welding on corrosion behavior of 316L stainless steel,” *Mater Lett*, 61(11-12): 2343-2346, (2007).
- [39] Scheuer C. J., Cardoso R. P., das Neves J. C. K., and Brunatto S. F., “Micro-abrasive wear behaviour of low-temperature plasma carburized aisi 420 martensitic stainless steel,” *Anais do Congresso Anual da ABM*, São Paulo, 391-405, (2017).
- [40] Filho M. V. M., Naeem M., Monção R. M., Díaz-Guillén J. C., Hdz-García H. M., Costa T. H. C., Safeen K., Iqbal J., Khan K. H., and Sousa R. R. M., “Improved mechanical and wear properties of AISI-420 steel by cathodic cage plasma vanadium nitride deposition,” *Phys Scr*, 98(11): 115602, (2023).
- [41] Trevisiol C., Jourani A., and Bouvier S., “Effect of hardness, microstructure, normal load and abrasive size on friction and on wear behaviour of 35NCD16 steel,” *Wear*, 388-389: 101-111, (2017).
- [42] Marenych O. O., Ding D., Pan Z., Kostyrychev A. G., Li H., and van Duin S., “Effect of chemical composition on microstructure, strength and wear resistance of wire deposited Ni-Cu alloys,” *Addit Manuf*, 24: 30-36, (2018).
- [43] Özer G., Khan H. M., Tarakçı G., Yılmaz M. S., Yaman P., Karabeyoğlu S. S., and Kısasöz A., “Effect of heat treatments on the microstructure and wear behaviour of a selective laser melted maraging steel,” *Proceedings of the Institution of Mechanical Engineers, Part E: Journal of Process Mechanical Engineering*, 236(6): 2526-2535, (2022).
- [44] Duman K., Karabeyoğlu S. S., and Yaman P., “Effect of nitriding conditions and operation temperatures on dry sliding wear properties of the aluminum extrusion die steel in the industry,” *Mater Today Commun*, 31: 103628, (2022).
- [45] Gu W., Chu K., Lu Z., Zhang G., and Qi S., “Synergistic effects of 3D porous graphene and T161 as hybrid lubricant additives on 316 ASS surface,” *Tribol Int*, 161: 107072, (2021).
- [46] Li D., Kong N., Zhang B., Zhang B., Li R., and Zhang Q., “Comparative study on the effects of oil viscosity on typical coatings for automotive engine components under simulated lubrication conditions,” *Diam Relat Mater*, 112: 108226, (2021).